THE JOURNAL OF BIOLOGICAL CHEMISTRY VOL. 287, NO. 4, pp. 2353–2363, January 20, 2012

Fibroblast Growth Factor 9 (FGF9)-Pituitary Homeobox 2 (PITX2) Pathway Mediates Transforming Growth Factor β (TGFβ) Signaling to Regulate Cell Proliferation in Palatal Mesenchyme during Mouse Palatogenesis*[S]

Received for publication, July 12, 2011, and in revised form, November 25, 2011 Published, JBC Papers in Press, November 28, 2011, DOI 10.1074/jbc.M111.280974

Jun-ichi Iwata[‡], Lily Tung[‡§], Mark Urata[‡§], Joseph G. Hacia[¶], Richard Pelikan[‡], Akiko Suzuki[‡], Liza Ramenzoni[‡], Obaid Chaudhry[‡§], Carolina Parada[‡], Pedro A. Sanchez-Lara[‖], and Yang Chai[‡1]**

*From the [‡]Center for Craniofacial Molecular Biology, Ostrow School of Dentistry, and [¶]Department of Biochemistry and Molecular Biology, Broad Center for Regenerative Medicine and Stem Cell Research, University of Southern California, Los Angeles, California 90033, the [‖]Department of Pediatrics and [§]Division of Plastic and Reconstruction Surgery, Keck School of Medicine, University of Southern California, Los Angeles, California 90089, and the **Division of Medical Genetics, Children's Hospital Los Angeles, Los Angeles, California 90027*

Cleft palate represents one of the most common congenital birth defects. Transforming growth factor β (TGFβ) signaling plays crucial functions in regulating craniofacial development, and loss of TGFβ receptor type II in cranial neural crest cells leads to craniofacial malformations, including cleft palate in mice (*Tgfbr2*$^{fl/fl}$;*Wnt1-Cre* mice). Here we have identified candidate target genes of TGFβ signaling during palatal formation. These target genes were selected based on combining results from gene expression profiles of embryonic day 14.5 palates from *Tgfbr2*$^{fl/fl}$;*Wnt1-Cre* mice and previously identified cleft palate phenotypes in genetically engineered mouse models. We found that fibroblast growth factor 9 (*Fgf9*) and transcription factor pituitary homeobox 2 (*Pitx2*) expressions are significantly down-regulated in the palate of *Tgfbr2*$^{fl/fl}$;*Wnt1-Cre* mice, and *Fgf9* and *Pitx2* loss of function mutations result in cleft palate in mice. *Pitx2* expression is down-regulated by siRNA knockdown of *Fgf9*, suggesting that *Fgf9* is upstream of *Pitx2*. We detected decreased expression of both cyclins D1 and D3 in the palates of *Tgfbr2*$^{fl/fl}$;*Wnt1-Cre* mice, consistent with the defect in cell proliferation. Significantly, exogenous FGF9 restores expression of cyclins D1 and D3 in a *Pitx2*-dependent manner and rescues the cell proliferation defect in the palatal mesenchyme of *Tgfbr2*$^{fl/fl}$;*Wnt1-Cre* mice. Our study indicates that a TGFβ-FGF9-PITX2 signaling cascade regulates cranial neural crest cell proliferation during palate formation.

Cleft palate represents one of the most frequent congenital birth defects in the human population (1). The causes of cleft palate remain largely unknown, but they appear to be complex, including genetic and environmental factors (2, 3). Cleft palate causes many clinical symptoms and complications, such as difficulties with suckling and eating, dysfunction of tongue and oral muscles, dental abnormalities, and speech and language delay (4). Therefore, prevention of cleft palate is the ultimate objective, and a prerequisite of this aim is to elucidate the mechanisms of healthy palate development and the causes of cleft palate.

The majority of cells in the craniofacial region are derived from cranial neural crest cells (CNCC),[2] which produce the facial skeleton, smooth muscle, and sensory nerve. Transforming growth factor β (TGFβ) signaling plays crucial functions in craniofacial development, including palate formation by mediating cell proliferation, differentiation, and extracellular matrix formation via regulation of downstream target genes (5–7). TGFβ ligands activate the membrane receptor serine/threonine kinase complex composed of TGFβ receptor type II (TβRII) and TGFβ receptor type I (TβRI/ALK5). The ligand-receptor complex phosphorylates SMAD2 and SMAD3, which form a transcriptional complex with SMAD4, and then the transcriptional complex translocates into the nucleus to control the expression of downstream target genes (8–10). TβRII is expressed in the CNCC-derived palatal mesenchyme (11, 12), and targeted null mutation of *Tgfbr2* in CNCC leads to craniofacial malformations, including small mandible, dysmorphic calvaria, and cleft palate (13–18). In humans, mutations in *TGFBR2* cause the multisystemic Loeys-Dietz syndrome (OMIM number 609192), which includes craniofacial malformations, such as cleft palate.

Our previous study showed that conditional gene ablation of *Tgfbr2* in CNCC (*Tgfbr2*$^{fl/fl}$;*Wnt1-Cre* mice) results in cleft palate with 100% phenotype penetrance, down-regulated cyclin D1 expression, and decreased CNCC proliferation in the palatal mesenchyme at embryonic day 14.5 (E14.5) (13). TGFβ signaling interacts with other growth factors, such as bone morphogenetic protein, Wnt, and fibroblast growth factor (FGF) (19). Although this interplay of pathways appears to be critical for the regulation of palate formation, little is known regarding the

* This work was supported, in whole or in part, by National Institutes of Health, NIDCR, Grants DE012711, DE014078, and DE017007 (to Y. C.).

[S] This article contains supplemental Tables 1–5 and Figs. 1–4.

[1] To whom correspondence should be addressed: Center for Craniofacial Molecular Biology, Ostrow School of Dentistry, University of Southern California, 2250 Alcazar St., CSA 103, Los Angeles, CA 90033. Tel.: 323-442-3480; Fax: 323-442-2981; E-mail: ychai@usc.edu.

[2] The abbreviations used are: CNCC, cranial neural crest cell(s); FDR, false discovery rate; MEPM, mouse embryonic palatal mesenchymal; TβRI, TβRII, and TβRIII, TGFβ receptor type I, II, and III, respectively; E13.5 and E14.5, embryonic day 13.5 and 14.5, respectively.

developmental molecular pathways that regulate cell proliferation during palatogenesis. Here we show that TGFβ regulates cell proliferation via the FGF9-PITX2 signaling cascade during palate formation.

EXPERIMENTAL PROCEDURES

Animals—Mating *Tgfbr2*$^{fl/+}$;*Wnt1-Cre* with *Tgfbr2*$^{fl/fl}$ mice generated *Tgfbr2*$^{fl/fl}$;*Wnt1-Cre* conditional null alleles that were genotyped using PCR primers as described previously (13). All mouse embryos used in this study were maintained in a C57BL/6J background. Animal usage was approved by the Institutional Animal Care and Use Committee at the University of Southern California.

Immunological Analysis—Immunoblots were performed as described previously (17). Antibodies used for immunoblotting were as follows: rabbit polyclonal antibodies against cyclin D1, cyclin D3, PITX2, and FGF9 (Cell Signaling Technology) and mouse monoclonal antibody against GAPDH (Chemicon).

Histological Examination—BrdU staining was performed as described previously (13, 14, 17). Immunohistochemical staining was performed as described previously (20, 21). Rabbit polyclonal antibodies used for immunohistochemistry were anti-cyclin D1 and anti-cyclin D3 (Cell Signaling Technology).

RNA Preparation and Quantitative RT-PCR—As described in a different analysis of these same samples,[3] total RNA was isolated from mouse embryonic palate dissected at the indicated developmental stage or from primary mouse embryonic palatal mesenchymal (MEPM) cells. First-strand cDNA was synthesized from 2 μg of total RNA using an oligo(dT)$_{20}$ primer and SuperScript III reverse transcriptase (Invitrogen). RNA was quantified and tested for quality by photometric measurement. Quantitative PCR was performed in triplicate by SYBR Green (Bio-Rad) in an iCycler (Bio-Rad) as previously described (17). A melting curve was obtained for each PCR product after each run to confirm that the SYBR Green signal corresponded to a unique and specific amplicon. The relative abundance of each transcript was calculated based on PCR efficiency and cycle number at which the fluorescence crosses a threshold for the GAPDH internal reference, and the gene was tested using iCycler iQ optical system software (Bio-Rad). PCR primers are available upon request.

Microarray Analysis—As described for these same samples,[3] total RNA samples (1 μg/sample) were converted into biotin-labeled cRNA using the GeneChip® IVT labeling kit and standard protocols recommended by Affymetrix (Santa Clara, CA). Fragmented cDNA was applied to GeneChip® mouse genome 430 2.0 arrays (Affymetrix) that contain probe sets designed to detect over 39,000 transcripts. Microarrays were hybridized, processed, and scanned, as described previously using the manufacturer's recommended conditions (22). WebArray software was used to generate scaled log2 transformed gene expression values using the RMA algorithm (23, 24). Probes sets showing >1.5-fold differential expression with a <5% false discovery rate (FDR) were identified through LIMMA (linear models for microarray data)-based linear model statistical analysis, and FDR calculations were made using the SPLOSH (spacings LOESS histogram) method. All scaled gene expression scores, and .cel files are available at the National Center for Biotechnology Information GEO (Gene Expression Omnibus) repository under series accession number GSE22989.

Comparative Analysis of Transcription Factor Binding Sites—We used the University of California Santa Cruz genome browser (available on the University of California Santa Cruz Web site) to obtain the genomic sequences of the human *FGF9* (RefSeq accession NM_002010.2) and *PITX2*, transcript variant 1 (RefSeq accession NM_153427.2) genes, including 5 kb upstream and 5 kb downstream of the respective transcription start sites, based on human genome Build 19. These sequences were then mapped to seven additional mammalian genomes (chimpanzee (Build 2.1.3), orangutan (Build 2.0.2), rhesus macaque (Build 1.0), mouse (Build 37), rat (Build 3.4), dog (Build 2), and horse (Build equCab2)) through the Blat tool (available on the University of Santa Cruz Web site). We obtained multiple alignments for these sequences using the ClustalW2 tool (available on the EMBL-EBI Web site) with default parameters and settings (25). To account for uncertainty in the quality of the horse and dog draft genome sequences, we performed sequence alignments with and without information from these species. We searched for transcription factor binding motifs relevant to SMAD and p38 MAPK pathway elements within or proximal to these genes (*i.e.* 5 kb upstream and 5 kb downstream of the human transcription start site for each gene) that are conserved across diverse mammals. We focused our analysis of canonical TGFβ signaling on the 5′-GTCT-3′, 5′-AGAC-3′, and 5′-GTCTAGAC-3′ SMAD recognition sites (26, 27). For our analysis of non-canonical TGFβ signaling, we focused on the well defined recognition sequences of ATF family members (5′-TGACGTCA-3′, as reported in Ref. 28) as well as that of ATF2 CRE-binding heterodimers, which recognize the 8-base sequence 5′-TGACGTAG-3′ (29) and related sequence variants 5′-TGACG(Y/M/R)-3′ (30, 31).

In Situ Hybridizations—*Fgf9* and *Pitx2* expression patterns in the palate were examined by *in situ* hybridization performed using methods described previously (14, 17). *Pitx2* and *Fgf9* probes were gifts from Drs. Liu and Thesleff, respectively (32, 33). Several negative controls (*e.g.* sense probe and no probe) were run in parallel with the experimental reaction. Cryosections were pretreated with proteinase K (Sigma), refixed in fresh 4% PFA, 0.2% glutaraldehyde in phosphate-buffered saline (PBS), and then prehybridized for 5 h at 55 °C in a hybridization buffer including 50% formamide. After hybridization, tissues were washed in high stringency conditions and preblocked in antibody blocking solution and then incubated with preabsorbed antibody. Color development was performed in nitro blue tetrazolium/5-bromo-4-chloro-3′-indolylphosphate color development solution (Sigma). Following visualization, the tissues were postfixed and cleared in 50% glycerol before photography.

Small Interfering RNA (siRNA) Transfection—MEPM cells (2×10^6 cells) were plated in a 6-well cell culture plate until the cells reached 60–80% confluence. siRNA duplex and reagents were purchased from Invitrogen and Santa Cruz Biotechnol-

[3] J. Iwata, J. G. Hacia, A. Suzuki, P. A. Sanchez-Lara, M. Urata, and Y. Chai, submitted for publication.

ogy, Inc. (Santa Cruz, CA), respectively. The siRNA mixture in transfection medium was incubated with cells for 6 h at 37 °C in a CO_2 incubator.

Organ Culture of Palate and FGF9 Bead Implantation—Timed pregnant mice were sacrificed at E13.5. Genotyping was carried out as described above. The palatal shelves were microdissected and cultured in serum-free chemically defined medium as described previously (13). To remove the epithelium, palatal shelves were treated with 0.05% trypsin, EDTA for 10 min prior to careful dissection. After 24 h in culture with p38 mitogen-activated protein kinase (MAPK) inhibitor SB203580 (100 μM), palates were harvested, fixed in 4% paraformaldehyde, 0.1 M phosphate buffer (pH 7.4), and processed. Heparin beads (Sigma) were used for delivery of FGF9 protein. The beads were washed in PBS and then incubated for 1 h at room temperature in 100 μg/ml FGF9 (R&D Systems). The FGF9-containing beads were delivered into palatal explants. Control beads were incubated with 0.1% bovine serum albumin (BSA). FGF9- or BSA-containing beads were placed into palatal explants.

Primary Cultured Cells Derived from Mouse Embryonic Palatal Mesenchyme—Primary MEPM cells were obtained from 13.5-day-old embryos. Palates were dissected at E13.5 and trypsinized for 30 min at 37 °C in a CO_2 incubator. After pipetting thoroughly, cells were cultured in Dulbecco's modified Eagle's medium containing 10% fetal bovine serum supplemented with penicillin, streptomycin, L-glutamate, sodium pyruvate, and non-essential amino acids. MEPM cells were treated with or without p38 MAPK inhibitor SB203580 at 10 μM for 24 h.

Statistical Analysis—Two-tailed Student's *t* test was applied for statistical analysis. For all graphs, data are represented as mean ± S.D. A p value of <0.05 was considered statistically significant.

RESULTS

Selection of TGFβ Downstream Signaling Molecules Crucial for Palatogenesis—To investigate the cause of cleft palate resulting from *TGFBR2* mutations in humans, we examined mice with CNCC-specific conditional inactivation of *Tgfbr2* (*Tgfbr2*$^{fl/fl}$;*Wnt1-Cre*). As will be described in detail,[4] we obtained gene expression profiles of E14.5 palate from *Tgfbr2*$^{fl/fl}$;*Wnt1-Cre* and *Tgfbr2*$^{fl/fl}$ control mice using Affymetrix U430 2.0 GeneChips (during palatal fusion, $n = 5$ per genotype). We chose this stage because it is the time at which normal mouse palatal fusion takes place. Overall, we found that a total of 293 transcripts were differentially expressed (149 were up-regulated, and 144 were down-regulated; ≥1.5-fold, <5% FDR) in *Tgfbr2*$^{fl/fl}$;*Wnt1-Cre* mice relative to the controls (Fig. 1*A*). Although TGFβ signaling interacts with other growth factors, such as bone morphogenetic protein, Wnt, and FGF family members, *Fgf9* was the only member of these growth factor families that was differentially expressed in E14.5 *Tgfbr2*$^{fl/fl}$;*Wnt1-Cre* palates relative to controls (1.52-fold down-regulated, FDR = 0.011).

[4] J. Iwata, R. Pelikan, Y. Chai, and J. G. Hacia, manuscript in preparation.

Next, we created a list of various genetically engineered mouse models known to exhibit the cleft palate phenotype during embryogenesis, as originally compiled by Mouse Genome Informatics (MGI) and modified by us based on the literature. Currently, this includes 277 different genetically engineered mice with cleft palate (Fig. 1*A* and supplemental Table 1). To screen for candidate genes related to cleft palate and TGFβ signaling, we compared the list of known mutant mouse models exhibiting cleft palate and the microarray analysis performed on E14.5 *Tgfbr2*$^{fl/fl}$;*Wnt1-Cre* palates. We identified two overlapping genes (*Fgf9* and *Pitx2*) in these lists (Fig. 1*A* and supplemental Table 1), which were both predicted to be less highly expressed in the palates of *Tgfbr2*$^{fl/fl}$;*Wnt1-Cre* mice relative to those of controls (*Fgf9*, 1.52-fold reduced, FDR = 0.011; *Pitx2*, 1.74-fold reduced, FDR = 0.006). *Fgf9*-null and *Pitx2*-null mice have been reported to show cleft palate (34, 35). We confirmed the reduction of *Fgf9* and *Pitx2* gene expression in *Tgfbr2*$^{fl/fl}$;*Wnt1-Cre* mice by quantitative RT-PCR using palates of *Tgfbr2*$^{fl/fl}$;*Wnt1-Cre* and *Tgfbr2*$^{fl/fl}$ control mice. Gene expression of both *Fgf9* and *Pitx2* was significantly down-regulated in *Tgfbr2*$^{fl/fl}$;*Wnt1-Cre* mice relative to control mice (Fig. 1*B*).

We performed *in situ* hybridization to investigate the expression patterns of *Fgf9* and *Pitx2* during palate formation. The expression of *Fgf9* was localized in the palatal epithelium in both *Tgfbr2*$^{fl/fl}$;*Wnt1-Cre* and *Tgfbr2*$^{fl/fl}$ control mice at E13.5 (Fig. 1*C*). At E14.5, *Fgf9* gene expression was detectable in both the palatal epithelium and mesenchyme in *Tgfbr2*$^{fl/fl}$ control mice; however, *Fgf9* gene expression was not detectable in the palatal mesenchyme of E14.5 *Tgfbr2*$^{fl/fl}$;*Wnt1-Cre* mice, although it remained detectable in the palatal epithelium (Fig. 1, *C* and *E*, and supplemental Fig. 1). *Pitx2* gene expression was detectable in the palatal epithelium of both *Tgfbr2*$^{fl/fl}$;*Wnt1-Cre* and *Tgfbr2*$^{fl/fl}$ control mice at E13.5 and E14.5. In *Tgfbr2*$^{fl/fl}$ control mice, *Pitx2* expression was also detectable in the palatal mesenchyme at E14.5 (Fig. 1, *D* and *F*, and supplemental Fig. 1). In E14.5 *Tgfbr2*$^{fl/fl}$;*Wnt1-Cre* mice, *Pitx2* expression was not detectable in the palatal mesenchyme (Fig. 1, *D* and *F*, and supplemental Fig. 1). The expression patterns were essentially the same for both *Fgf9* and *Pitx2*. We also analyzed FGF9 and PITX2 protein expression in the palates of *Tgfbr2*$^{fl/fl}$;*Wnt1-Cre* and *Tgfbr2*$^{fl/fl}$ control mice at E14.5 and found that they were both reduced in *Tgfbr2*$^{fl/fl}$;*Wnt1-Cre* palates (Fig. 1*G* and supplemental Fig. 2).

Fgf9 Regulates Pitx2 Gene Expression via SMAD-independent TGFβ Signaling during Palate Formation—Here, we investigated the means by which TGFβ regulated *Fgf9* and *Pitx2* expressions. There are at least two possibilities; one is through the non-canonical TGFβ signaling (such as p38 MAPK activation), and another is through the canonical SMAD-dependent pathway. Our recent study showed that loss of *Tgfbr2* in CNCC resulted in an activation of an alternative TGFβ signaling cascade that involved the activation of p38 MAPK.[3] We hypothesized that blocking p38 MAPK activation will restore the gene expression of *Fgf9* and *Pitx2* in the palatal mesenchyme of *Tgfbr2*$^{fl/fl}$;*Wnt1-Cre* mice. To test this, we analyzed *Fgf9* and *Pitx2* gene expression after treatment with p38 MAPK inhibitor SB203580 using primary MEPM cells derived from the palates of *Tgfbr2*$^{fl/fl}$;*Wnt1-Cre* and *Tgfbr2*$^{fl/fl}$ control mice. We found

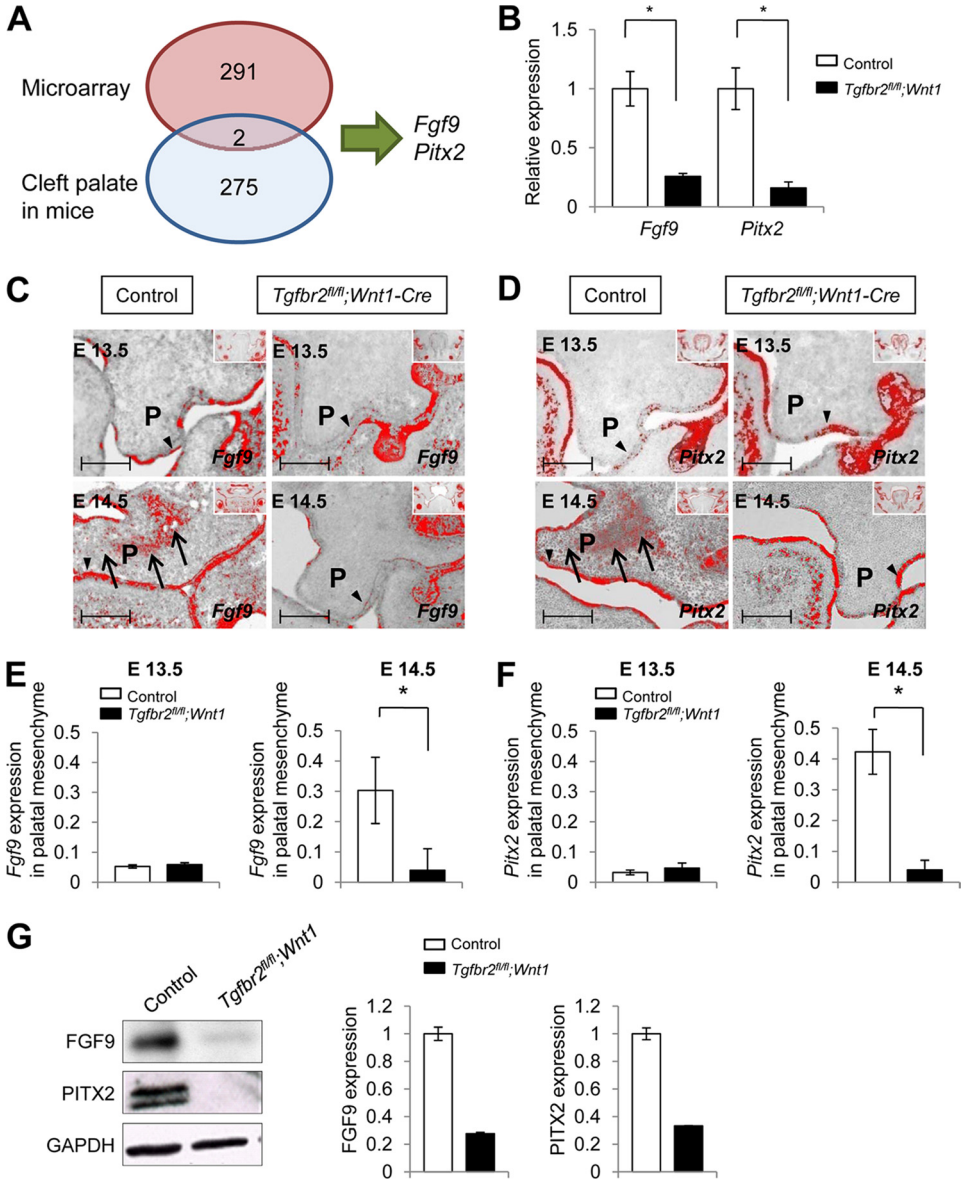

FIGURE 1. ***Fgf9* and *Pitx2* are down-regulated in *Tgfbr2*$^{fl/fl}$;*Wnt1-Cre* mice at E14.5.** *A*, diagram depicts the strategy used to identify *Fgf9* and *Pitx2* genes in our approach using the combination of E14.5 palate microarray analysis and known mutations in mice that result in cleft palate phenotypes. *B*, quantitative RT-PCR analysis of *Fgf9* and *Pitx2* in *Tgfbr2*$^{fl/fl}$;*Wnt1-Cre* (*closed columns*) mice compared with *Tgfbr2*$^{fl/fl}$ control mice (*open columns*) in the palate at E14.5. *, $p < 0.05$. *C* and *D*, *in situ* hybridization of *Fgf9* (*C*) and *Pitx2* (*D*) in *Tgfbr2*$^{fl/fl}$;*Wnt1-Cre* and *Tgfbr2*$^{fl/fl}$ mice at E13.5 and E14.5. The *arrows* indicate expression of *Fgf9* and *Pitx2* in the palatal mesenchyme of *Tgfbr2*$^{fl/fl}$ control mice. *Arrowheads*, *Fgf9* and *Pitx2* expression in the palatal epithelium of *Tgfbr2*$^{fl/fl}$ control and *Tgfbr2*$^{fl/fl}$;*Wnt1-Cre* mice. *Insets* show low magnification of craniofacial regions to indicate global expression pattern of *Fgf9* and *Pitx2*. *P*, palatal shelf. *Bar*, 50 μm. *E* and *F*, quantitative RT-PCR analysis of *Fgf9* (*E*) and *Pitx2* (*F*) in the palatal mesenchyme of E13.5 and E14.5 *Tgfbr2*$^{fl/fl}$ control (*open columns*) and *Tgfbr2*$^{fl/fl}$;*Wnt1-Cre* (*closed columns*) mice. *, $p < 0.05$. *G*, immunoblotting analysis of FGF9 and PITX2 in E14.5 *Tgfbr2*$^{fl/fl}$ control and *Tgfbr2*$^{fl/fl}$;*Wnt1-Cre* palates. The graph shows quantitative densitometry analysis of the immunoblotting data. *Error bars*, S.D.

that *Fgf9* and *Pitx2* expression increased in *Tgfbr2*$^{fl/fl}$;*Wnt1-Cre* MEPM cells treated with p38 MAPK inhibitor to a level comparable with that of *Tgfbr2*$^{fl/fl}$ control MEPM cells, consistent with *Fgf9* and *Pitx2* down-regulation by p38 MAPK activation in the absence of *Tgfbr2* (Fig. 2*A*). Moreover, we added p38 MAPK inhibitor to an *ex vivo* palate organ culture system and confirmed that gene expression of *Fgf9* and *Pitx2* in *Tgfbr2*$^{fl/fl}$;*Wnt1-Cre* palates increased after treatment (Fig. 2*B* and supplemental Fig. 3).

Next, to explore the mechanism by which *Fgf9* and *Pitx2* interact with each other during palate development, we reduced the gene expression of *Fgf9* or *Pitx2* in primary MEPM cells using a siRNA knockdown approach (Fig. 2, *C–F*). Gene expression of *Fgf9* and *Pitx2* was successfully suppressed by the siRNA treatment by 73 and 54%, respectively (Fig. 2, *C* and *E*). We found that gene expression of *Pitx2* was significantly decreased 3.5-fold after *Fgf9* siRNA treatment, but *Pitx2* siRNA treatment had no effect on gene expression of *Fgf9* (Fig. 2, *D* and *F*). These data suggest that *Fgf9* may regulate the gene expression of *Pitx2* in the palatal mesenchyme during palatogenesis.

TGFβ Signaling Regulates Expression of Cyclins D1 and D3 via SMAD-independent Pathway during Palate Formation—Our previous work demonstrated that cyclin D1 expression is down-regulated in the palatal mesenchyme in *Tgfbr2*$^{fl/fl}$;*Wnt1-*

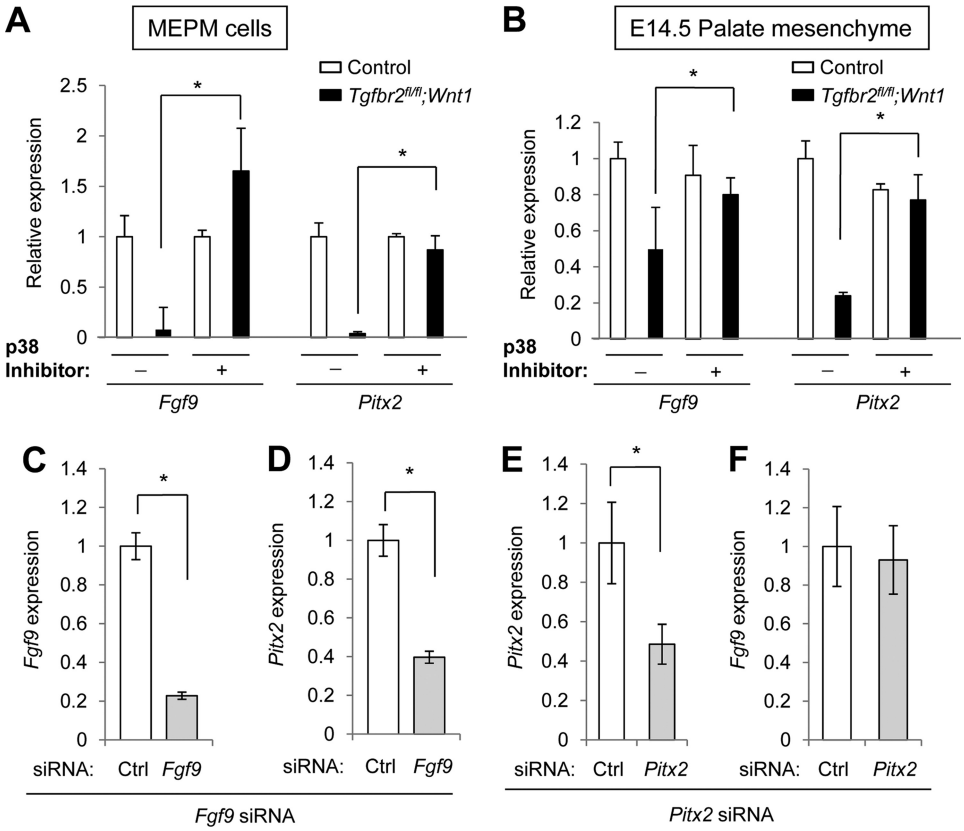

FIGURE 2. **Fgf9 regulates the gene expression of *Pitx2*.** *A*, quantitative RT-PCR analysis of *Fgf9* and *Pitx2* after treatment (+) or no treatment (−) with p38 MAPK inhibitor of primary MEPM cells from *Tgfbr2*$^{fl/fl}$ control (*open columns*) and *Tgfbr2*$^{fl/fl}$;*Wnt1-Cre* (*closed columns*) mice. *, $p < 0.05$. *B*, quantitative RT-PCR analysis of *Fgf9* and *Pitx2* after treatment (+) or no treatment (−) with p38 MAPK inhibitor in organ culture of E14.5 palatal mesenchyme from *Tgfbr2*$^{fl/fl}$ control (*open columns*) and *Tgfbr2*$^{fl/fl}$;*Wnt1-Cre* (*closed columns*) mice. *, $p < 0.05$. *C* and *D*, gene expressions of *Fgf9* (*C*) and *Pitx2* (*D*) after siRNA knockdown of *Fgf9* in primary MEPM cells from *Tgfbr2*$^{fl/fl}$ mice. *, $p < 0.05$. Antisense siRNA treatment was used as control (*Ctrl*). *, $p < 0.05$. *E* and *F*, gene expression of *Fgf9* (*E*) and *Pitx2* (*F*) after siRNA knockdown for *Pitx2* in primary MEPM cells from *Tgfbr2*$^{fl/fl}$ mice. *, $p < 0.05$. Antisense siRNA treatment was used as control (*Ctrl*). *Error bars*, S.D.

Cre mice at E14.5 (13). Therefore, we investigated the gene expression of cyclin D isoforms at E14.5 and found that both cyclins D1 and D3 were significantly down-regulated in palates from E14.5 *Tgfbr2*$^{fl/fl}$;*Wnt1-Cre* mice (Fig. 3*A*). Cyclins D1 and D3 protein levels were also down-regulated in *Tgfbr2*$^{fl/fl}$;*Wnt1-Cre* palates at E14.5 (Fig. 3*B*). Furthermore, we detected cyclin D3 in the palatal mesenchyme of E14.5 *Tgfbr2*$^{fl/fl}$ control mice, but we failed to detect them in the palates of *Tgfbr2*$^{fl/fl}$;*Wnt1-Cre* mice at E14.5 (Fig. 3*C*). Significantly, decreased gene expression of *Ccnd1* and *Ccnd3* in *Tgfbr2*$^{fl/fl}$;*Wnt1-Cre* MEPM cells was restored by treatment with p38 MAPK inhibitor SB203580, suggesting that the SMAD-independent p38 MAPK pathway regulates gene expression of *Ccnd1* and *Ccnd3* in *Tgfbr2*$^{fl/fl}$;*Wnt1-Cre* mice (Fig. 4*A*).

To investigate the role of FGF9 in TGFβ-mediated cell proliferation during palate formation, we analyzed the gene expression of cyclins D1 and D3 after treatment with FGF9 protein using the *ex vivo* palate organ culture system. Decreased gene expression of cyclins D1 and D3 in *Tgfbr2*$^{fl/fl}$;*Wnt1-Cre* palate was restored to control levels after FGF9 treatment (Fig. 4*B*). Protein levels of cyclins D1 and D3 were also restored after FGF9 treatment in *Tgfbr2*$^{fl/fl}$;*Wnt1-Cre* palates (Fig. 4*C*).

Next, we investigated the possible requirement for *Pitx2* during FGF9 induction of *Ccnd1* and *Ccnd3* expression. As described above, gene expression of *Ccnd1* and *Ccnd3* was induced by FGF9 treatment in *Tgfbr2*$^{fl/fl}$;*Wnt1-Cre* MEPM cells; however, *Ccnd1* and *Ccnd3* expression was not induced by FGF9 treatment following siRNA knockdown of *Pitx2* (Fig. 4, *D* and *E*). These data again indicate that *Pitx2* is a downstream target for FGF9 and show that *Pitx2* is required for FGF9-mediated induction of *Ccnd1* and *Ccnd3* expression. Taken together, our results demonstrate that expression of cyclins D1 and D3 is regulated by a TGFβ-FGF9-PITX2 signaling pathway.

FGF9 Rescues the Cell Proliferation Defect in Tgfbr2$^{fl/fl}$*;Wnt1-Cre Mice via Pitx2*—We investigated whether the cell proliferation defect in *Tgfbr2*$^{fl/fl}$;*Wnt1-Cre* mice was rescued by the addition of FGF9. First, we treated MEPM cells with exogenous FGF9 and found that gene expression of *Pitx2* in *Tgfbr2*$^{fl/fl}$;*Wnt1-Cre* MEPM cells was increased to that of control *Tgfbr2*$^{fl/fl}$ MEPM cells (Fig. 5*A*). We also implanted FGF9 or BSA beads in palates from *Tgfbr2*$^{fl/fl}$;*Wnt1-Cre* mice. FGF9-beads induced gene expression of *Pitx2* in *Tgfbr2*$^{fl/fl}$;*Wnt1-Cre* palates (Fig. 5, *B–D*). Thus, FGF9 can induce expression of *Pitx2* both *in vitro* and *ex vivo* in *Tgfbr2*$^{fl/fl}$;*Wnt1-Cre* mice. Furthermore, FGF9 treatment resulted in restored cell proliferation in the palate of *Tgfbr2*$^{fl/fl}$;*Wnt1-Cre* mice (Fig. 6, *A* and *B*). These data demonstrate that FGF9 can induce *Pitx2* expression and cell proliferation in the absence of TβRII. Thus, our results suggest that the FGF9-PITX2 pathway mediates TGFβ signal-

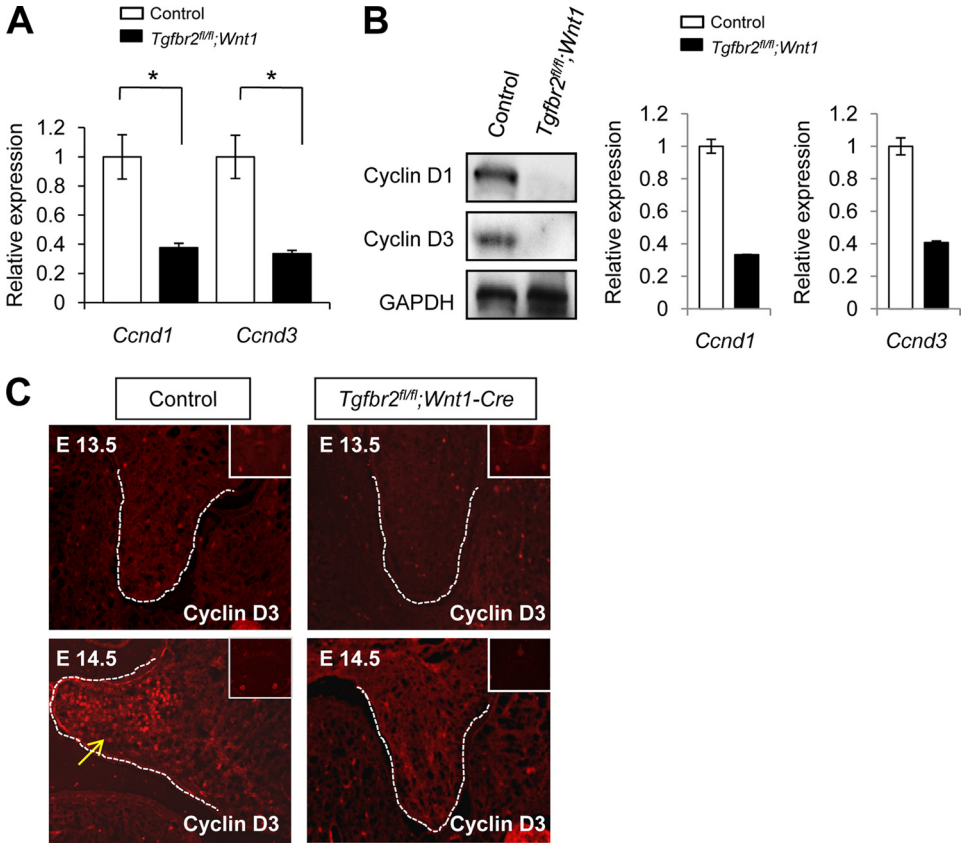

FIGURE 3. **Expression of cyclins D1 and D3 is decreased in *Tgfbr2*$^{fl/fl}$;*Wnt1-Cre* mice during palatal development.** *A*, quantitative RT-PCR analysis of cyclins D1 and D3 (*Ccnd1* and *Ccnd3*) in the palate of *Tgfbr2*$^{fl/fl}$ control (*open columns*) and *Tgfbr2*$^{fl/fl}$;*Wnt1-Cre* (*closed columns*) mice. *, $p < 0.05$. *B*, Western blot of cyclins D1 and D3 (*Ccnd1* and *Ccnd3*) in the palate of *Tgfbr2*$^{fl/fl}$ control and *Tgfbr2*$^{fl/fl}$;*Wnt1-Cre* mice at E14.5. The graph shows quantitative densitometry analysis of the immunoblotting data. *C*, immunohistochemical analysis of cyclin D3 in the palate of *Tgfbr2*$^{fl/fl}$ control and *Tgfbr2*$^{fl/fl}$;*Wnt1-Cre* mice at E13.5 and E14.5. The *arrows* indicate expression of cyclin D3 in the palatal mesenchyme of *Tgfbr2*$^{fl/fl}$ mice at E14.5. *Dotted lines*, palate. *Insets*, low magnification of craniofacial regions to indicate global expression pattern of cyclin D3. *Error bars*, S.D.

ing to contribute to mesenchymal cell proliferation during palatal formation (supplemental Fig. 4).

Phylogenetically Conserved SMAD and ATF2 Recognition Sequences Exist Proximal to or within the Human FGF9 and PITX2 Genes—We analyzed sequences of the human *FGF9* and *PITX2* genes (5-kb upstream and 5-kb downstream of their transcription start sites, respectively) and found that the *FGF9* genomic region has 69 potential SMAD recognition sites (15 of which were conserved in at least six mammals) and one potential ATF2 recognition site that was conserved in all eight mammalian genomes investigated (supplemental Tables 2 and 3). We focused on the ATF2 transcription factor because it is known to be regulated by the p38 MAPK pathway (36). The interrogated human *PITX2* genomic region had 65 potential SMAD recognition sites (seven of which were conserved in at least six mammals) and no ATF2 recognition sites (supplemental Tables 4 and 5). However, we found one ATF2 recognition site that was 5,032 bp downstream of the human *PITX2* transcription start site that was conserved in all eight mammalian genomes investigated. Although this focused analysis does not preclude the existence of other potential transcription factor binding sites relevant to non-canonical TGFβ signaling, it is conceivable that canonical SMAD-mediated TGFβ signaling may promote *Fgf9* expression, whereas non-canonical p38 MAPK-mediated signaling inhibits *Fgf9* expression.

DISCUSSION

TGFβ Signaling Is Crucial in Regulating Craniofacial Development—Heterozygous mutations in *TGFBR1* or *TGFBR2* are associated with Loeys-Dietz syndrome, which can manifest with craniofacial malformations, such as cleft palate, craniosynostosis, and hypertelorism; skeletal defects, such as scoliosis, arachnodactaly, and joint laxity; and vascular problems, including arterial tortuosity with the potential for aneurysms and dissections (37–39). In addition, heterozygous mutations in *FBN-1*, which encodes an elastic extracellular matrix protein called fibrillin-1, lead to excessive TGFβ signaling and cause Marfan syndrome, which exhibits clinical phenotypes similar to Loeys-Dietz syndrome (40–42). Furthermore, DiGeorge syndrome, which results from a variably sized deletion on chromosome 22 (del22q11), including about 30 genes, such as the transcription factor *Tbx1* and the signal adaptor protein *CrkL*, exhibits altered TGFβ signaling in ~80% of patients who have cleft palate and other craniofacial malformations (43–45). Thus, TGFβ signaling is crucial in regulating palate formation during embryonic development, and altered TGFβ signaling can lead to multiple human syndromes.

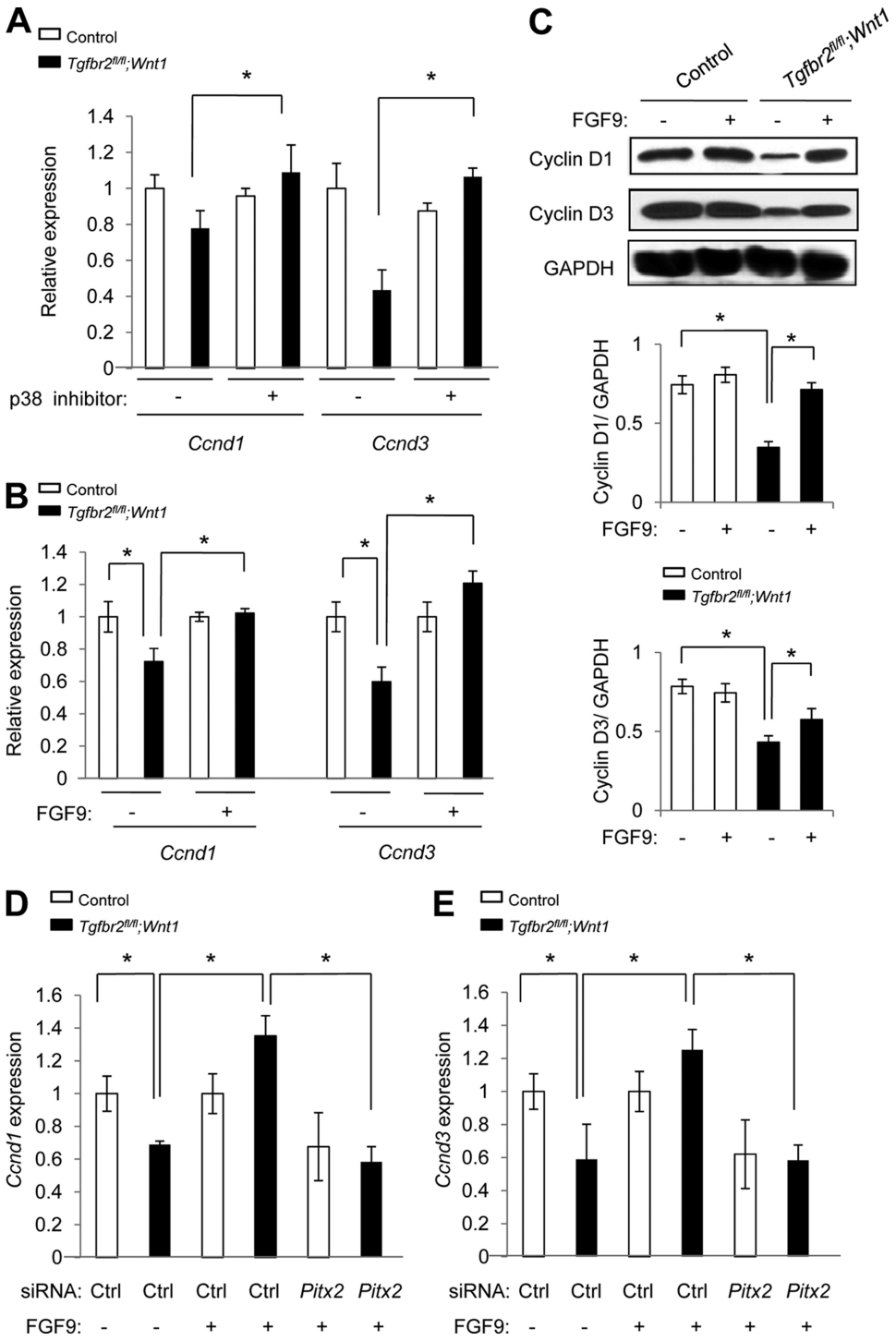

FIGURE 4. **TGFβ-mediated FGF9-PITX2 signaling regulates gene expression of *Ccnd1* and *Ccnd3* in palatal mesenchymal cells.** *A*, quantitative RT-PCR analysis of cyclins D1 (*Ccnd1*) and D3 (*Ccnd3*) in MEPM cells of *Tgfbr2*$^{fl/fl}$ control (*open columns*) and *Tgfbr2*$^{fl/fl}$;*Wnt1-Cre* (*closed columns*) mice with (+) or without (−) p38 MAPK inhibitor. *, $p < 0.05$. *B*, quantitative RT-PCR analysis of cyclins D1 and D3 in primary MEPM cells of *Tgfbr2*$^{fl/fl}$ control (*open columns*) and *Tgfbr2*$^{fl/fl}$;*Wnt1-Cre* (*closed columns*) mice after treatment (+) or no treatment (−) with FGF9 protein. *, $p < 0.05$. *C*, Western blots of cyclins D1 and D3 after treatment (+) or no treatment (−) with FGF9 protein. The graphs (*below*) show quantitative densitometry analysis of the immunoblotting data. *, $p < 0.05$. *D* and *E*, quantitative RT-PCR analysis of cyclins D1 (*D*; *Ccnd1*) and D3 (*E*; *Ccnd3*) in MEPM cells of *Tgfbr2*$^{fl/fl}$ control (*open columns*) and *Tgfbr2*$^{fl/fl}$;*Wnt1-Cre* (*closed columns*) mice after mock treatment (*Ctrl*), treatment with FGF9 protein (+), or treatment with a combination of FGF9 protein and siRNA for *Pitx2* for 24 h. *, $p < 0.05$. *Error bars*, S.D.

The utility of animal models with cleft palate is impressive, because multiple studies have begun to elucidate the cellular and molecular mechanisms of palate formation. In some cases, the human gene deficiency was identified first and replicated in an animal model, but in other cases, animal models provided leads to understanding the molecular mechanism of clinical syndromes. Now, over 200 genetically mutated mice exhibit cleft palate, and ~400 known human syndromes exhibit cleft palate as one of their clinical symptoms. Human gene linkage studies have shown that point mutations in *TGFBR1* or

TGFBR2 cause craniofacial deformities, such as cleft palate (37–39). Our strategy of identifying TGFβ downstream signaling molecules that are also crucial for palatogenesis will advance our understanding of the signaling network involved in regulating palate development in mice and humans.

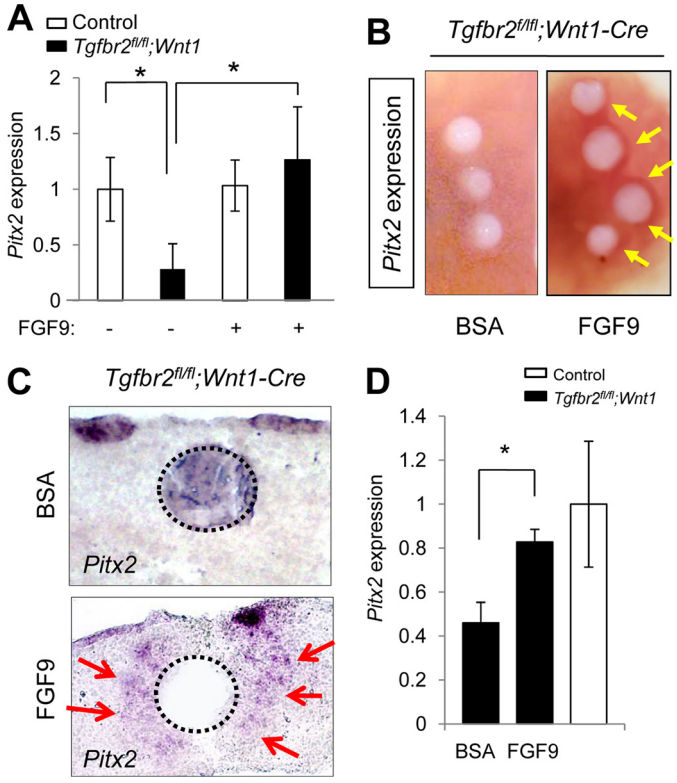

FIGURE 5. **Exogenous FGF9 rescues *Pitx2* expression in *Tgfbr2*$^{fl/fl}$;*Wnt1-Cre* mice during palatal development.** *A*, Quantitative RT-PCR analysis of *Pitx2* in primary MEPM cells of *Tgfbr2*$^{fl/fl}$ control (*open columns*) and *Tgfbr2*$^{fl/fl}$;*Wnt1-Cre* (*closed columns*) mice after treatment (+) or no treatment (−) with FGF9 protein. *, $p < 0.05$. *B*, whole mount *in situ* hybridization after implantation of FGF9 or BSA control beads in the palate of *Tgfbr2*$^{fl/fl}$;*Wnt1-Cre* mice. The *arrows* indicate the increased expression of *Pitx2* around FGF9 beads. *C*, section *in situ* hybridization for *Pitx2* after implantation of FGF9 or BSA control beads in the palate of the *Tgfbr2*$^{fl/fl}$;*Wnt1-Cre* mice. The *arrows* indicate the increased expression of *Pitx2* around FGF9 beads. *Dotted lines*, perimeter of the beads. *D*, quantitative RT-PCR analysis of *Pitx2* in the mesenchyme of *Tgfbr2*$^{fl/fl}$;*Wnt1-Cre* (*closed columns*) and *Tgfbr2*$^{fl/fl}$ control (*open column*) mice after FGF9 or BSA treatment. *, $p < 0.05$. *Error bars*, S.D.

TGFβ Signaling Regulates Fgf9 and Pitx2 Gene Expression—The FGF family includes 18 receptor-binding ligands and four FGF receptors (46). Among the FGF ligands, FGF9 can induce osteoblast proliferation and new bone formation (47, 48). *Fgf9*-null mice die at birth due to lung hypoplasia, and ~40% of *Fgf9*$^{-/-}$ embryos exhibit cleft palate (34). Interestingly, FGF9 can induce *Pitx2* expression in the mesenchyme derived from small intestine and lung (49, 50). The loss of TGFβ2 disrupts the expression of the causative genes for developmental glaucoma, *Foxc1* and *Pitx2* (51). Patients with *TGFBR2* or *TGFBR1* mutations show craniofacial defects and signs of elevated TGFβ signaling (38, 52, 53). Similarly, mutations in TGFβ receptor gene family members cause craniofacial deformities in mice (13, 54). However, it was unknown whether TGFβ ligands may still signal in *Tgfbr2* mutant mice. Our recent study showed that loss of *Tgfbr2* in CNCC results in elevated TGFβ2 and TβRIII expression, activation of a TβRI/TβRIII-mediated, SMAD-independent signaling pathway, and a cell proliferation defect in the palatal mesenchyme.[3] Strikingly, *Tgfb2*, *Tgfbr1/Alk5*, or *Tak1* haploinsufficiency disrupts TβRI/TβRIII-mediated signaling and rescues craniofacial deformities in *Tgfbr2* mutant mice, indicating that the activation of this non-canonical TGFβ signaling pathway is responsible for craniofacial malformations in *Tgfbr2* mutant mice.[3] In this study, we treated MEPM cells and palatal mesenchyme with a p38 MAPK inhibitor, and we found that gene expression of *Fgf9* was restored after the treatment with p38 MAPK inhibitor. These results indicate that non-canonical TGFβ-mediated p38 MAPK signaling regulates gene expression of *Fgf9* during palate formation. Furthermore, the presence of highly conserved candidate SMAD and ATF2 recognition sites proximal to or within the human *FGF9* and *PITX2* genes (supplemental Tables 2–5) provides preliminary evidence suggesting that a TGFβ2-FGF9-PITX2 signaling cascade could be a well conserved mechanism in regulating mammalian organogenesis.

Multiple studies have demonstrated that PITX2 has diverse roles in cell proliferation, differentiation, hematopoiesis, and organogenesis (32, 55–60). During early embryogenesis, PITX2 is a key regulator in the establishment of embryonic left-right asymmetry (61). At a later embryonic stage, PITX2 regulates

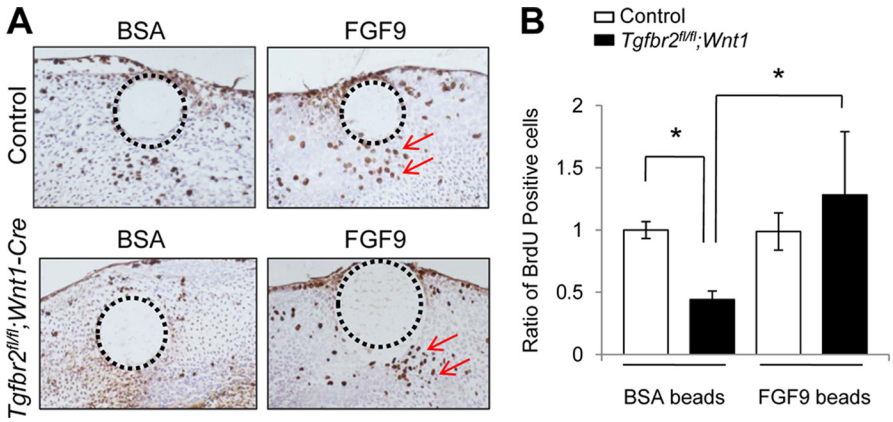

FIGURE 6. **Exogenous FGF9 rescues the cell proliferation defect of *Tgfbr2*$^{fl/fl}$;*Wnt1-Cre* mice during palatal development.** *A*, BrdU staining after treatment with FGF9 or BSA beads in the palate of *Tgfbr2*$^{fl/fl}$ control and *Tgfbr2*$^{fl/fl}$;*Wnt1-Cre* mice. The *arrows* indicate BrdU-positive cells. *Dotted lines*, perimeter of the beads. *B*, quantitative analysis of BrdU-positive cells in *A*. BrdU-positive cells were significantly increased in the palate of *Tgfbr2*$^{fl/fl}$;*Wnt1-Cre* mice after the treatment with FGF9-containing beads. *, $p < 0.05$. *Error bars*, S.D.

cell type-specific cell proliferation in response to growth factors during the development of the cardiac outflow tract (58). PITX2 is required for the differentiation of neural crest cells (51). Previous studies have also shown that PITX2 cooperates with β-catenin and LEF/TCF to regulate cell proliferation by directly activating transcription of cyclin Ds and c-Myc (51, 62). Our data indicate that PITX2 is downstream of TGFβ and FGF signaling and may also regulate cell proliferation by directly activating cyclin D1 and D3 gene expression. *Pitx2*-deficient mice die at an embryonic stage and show severe defects in heart, eye, pituitary gland, palate, and tooth development (35, 58). In addition, *PITX2* mutations have been identified in several human disorders, such as Axenfeld-Rieger syndrome, iridoniodysgenesis syndrome, and sporadic Peter syndrome (63–65). Some patients with these syndromes exhibit cleft palate among their defects.

We have previously reported that TGFβ signaling regulates FGF signaling in frontal bone development, and FGF2-containing beads rescue a defect in cell proliferation in frontal bone primordium in *Tgfbr2*$^{fl/fl}$;*Wnt1-Cre* mice (14). In the current study, we rescued a defect in cell proliferation in *Tgfbr2*$^{fl/fl}$;*Wnt1-Cre* palates by the addition of FGF9 *ex vivo* during palate development. Thus, TGFβ-mediated FGF signaling may be an important mechanism to regulate cell proliferation during embryogenesis.

Mice with neural crest cell-specific deletion of *Tgfbr2* (*Tgfbr2*$^{fl/fl}$;*Wnt1-Cre*) are useful for the investigation of craniofacial anomalies, such as cleft palate, because *Tgfbr2*$^{fl/fl}$;*Wnt1-Cre* mice exhibit craniofacial deformities, including cleft palate, at 100% penetrance (13, 17, 18, 66, 67). In addition, the defects in *Tgfbr2*$^{fl/fl}$;*Wnt1-Cre* embryos mimic defects in patients with Loeys-Dietz and DiGeorge syndromes (13, 45). Therefore, identification of downstream targets of TGFβ signaling, such as *Fgf9* and *Pitx2*, may be informative for future prevention, early diagnosis, and treatment of congenital birth defects.

Acknowledgments—We thank Julie Mayo for critical reading of the manuscript. We thank Dr. Harold Moses for Tgfbr2$^{fl/fl}$ *mice, Dr. Harold Slavkin for discussion, and the Microarray Core Facility of Children's Hospital Los Angeles for technical assistance.*

REFERENCES

1. Tolarová, M. M., and Cervenka, J. (1998) Classification and birth prevalence of orofacial clefts. *Am. J. Med. Genet.* **75,** 126–137
2. Mossey, P. A., Little, J., Munger, R. G., Dixon, M. J., and Shaw, W. C. (2009) Cleft lip and palate. *Lancet* **374,** 1773–1785
3. Yu, W., Serrano, M., Miguel, S. S., Ruest, L. B., and Svoboda, K. K. (2009) Cleft lip and palate genetics and application in early embryological development. *Indian J. Plast. Surg.* **42,** (suppl.) S35–S50
4. Ciminello, F. S., Morin, R. J., Nguyen, T. J., and Wolfe, S. A. (2009) Cleft lip and palate. Review. *Compr. Ther.* **35,** 37–43
5. Shah, N. M., Groves, A. K., and Anderson, D. J. (1996) Alternative neural crest cell fates are instructively promoted by TGFβ superfamily members. *Cell.* **85,** 331–343
6. Dorsky, R. I., Moon, R. T., and Raible, D. W. (2000) Environmental signals and cell fate specification in premigratory neural crest. *BioEssays.* **22,** 708–716
7. Nomura, M., and Li, E. (1998) Smad2 role in mesoderm formation, left-right patterning, and craniofacial development. *Nature.* **393,** 786–790
8. Heldin, C. H., Miyazono, K., and ten Dijke, P. (1997) TGF-β signaling from cell membrane to nucleus through SMAD proteins. *Nature.* **390,** 465–471
9. Massagué, J. (1998) TGF-β signal transduction. *Annu. Rev. Biochem.* **67,** 753–791
10. Pelton, R. W., Hogan, B. L., Miller, D. A., and Moses, H. L. (1990) Differential expression of genes encoding TGFs β 1, β 2, and β 3 during murine palate formation. *Dev. Biol.* **141,** 456–460
11. Cui, X. M., Warburton, D., Zhao, J., Crowe, D. L., and Shuler, C. F. (1998) Immunohistochemical localization of TGF-β type II receptor and TGF-β3 during palatogenesis *in vivo* and *in vitro*. *Int. J. Dev. Biol.* **42,** 817–820
12. Wang, Y. Q., Sizeland, A., Wang, X. F., and Sassoon, D. (1995) Restricted expression of type-II TGF β receptor in murine embryonic development suggests a central role in tissue modeling and CNS patterning. *Mech. Dev.* **52,** 275–289
13. Ito, Y., Yeo, J. Y., Chytil, A., Han, J., Bringas, P., Jr., Nakajima, A., Shuler, C. F., Moses, H. L., and Chai, Y. (2003) Conditional inactivation of Tgfbr2 in cranial neural crest causes cleft palate and calvaria defects. *Development* **130,** 5269–5280
14. Sasaki, T., Ito, Y., Bringas, P., Jr., Chou, S., Urata, M. M., Slavkin, H., and Chai, Y. (2006) TGFβ-mediated FGF signaling is crucial for regulating cranial neural crest cell proliferation during frontal bone development. *Development* **133,** 371–381
15. Oka, S., Oka, K., Xu, X., Sasaki, T., Bringas, P., Jr., and Chai, Y. (2007) Cell autonomous requirement for TGF-β signaling during odontoblast differentiation and dentin matrix formation. *Mech. Dev.* **124,** 409–415
16. Oka, K., Oka, S., Sasaki, T., Ito, Y., Bringas, P., Jr., Nonaka, K., and Chai, Y. (2007) The role of TGF-β signaling in regulating chondrogenesis and osteogenesis during mandibular development. *Dev. Biol.* **303,** 391–404
17. Iwata, J., Hosokawa, R., Sanchez-Lara, P. A., Urata, M., Slavkin, H., and Chai, Y. (2010) Transforming growth factor-β regulates basal transcriptional regulatory machinery to control cell proliferation and differentiation in cranial neural crest-derived osteoprogenitor cells. *J. Biol. Chem.* **285,** 4975–4982
18. Hosokawa, R., Oka, K., Yamaza, T., Iwata, J., Urata, M., Xu, X., Bringas, P., Jr., Nonaka, K., and Chai, Y. (2010) TGF-β mediated FGF10 signaling in cranial neural crest cells controls development of myogenic progenitor cells through tissue-tissue interactions during tongue morphogenesis. *Dev. Biol.* **341,** 186–195
19. Massagué, J. (2000) How cells read TGF-β signals. *Nat. Rev. Mol. Cell Biol.* **1,** 169–178
20. Iwata, J., Ezaki, J., Komatsu, M., Yokota, S., Ueno, T., Tanida, I., Chiba, T., Tanaka, K., and Kominami, E. (2006) Excess peroxisomes are degraded by autophagic machinery in mammals. *J. Biol. Chem.* **281,** 4035–4041
21. Sou, Y. S., Waguri, S., Iwata, J., Ueno, T., Fujimura, T., Hara, T., Sawada, N., Yamada, A., Mizushima, N., Uchiyama, Y., Kominami, E., Tanaka, K., and Komatsu, M. (2008) The Atg8 conjugation system is indispensable for proper development of autophagic isolation membranes in mice. *Mol. Biol. Cell.* **19,** 4762–4775
22. Karaman, M. W., Houck, M. L., Chemnick, L. G., Nagpal, S., Chawannakul, D., Sudano, D., Pike, B. L., Ho, V. V., Ryder, O. A., and Hacia, J. G. (2003) Comparative analysis of gene-expression patterns in human and African great ape cultured fibroblasts. *Genome Res.* **13,** 1619–1630
23. Xia, X., McClelland, M., and Wang, Y. (2005) WebArray. An online platform for microarray data analysis. *BMC Bioinformatics* **6,** 306
24. Wang, Y., McClelland, M., and Xia, X. Q. (2009) Analyzing microarray data using WebArray. *Cold Spring Harb. Protoc.* 2009, pdb.prot5260
25. Larkin, M. A., Blackshields, G., Brown, N. P., Chenna, R., McGettigan, P. A., McWilliam, H., Valentin, F., Wallace, I. M., Wilm, A., Lopez, R., Thompson, J. D., Gibson, T. J., and Higgins, D. G. (2007) ClustalW and ClustalX version 2.0. *Bioinformatics* **23,** 2947–2948
26. Denissova, N. G., Pouponnot, C., Long, J., He, D., and Liu, F. (2000) Transforming growth factor β-inducible independent binding of SMAD to the Smad7 promoter. *Proc. Natl. Acad. Sci. U.S.A.* **97,** 6397–6402
27. Zawel, L., Dai, J. L., Buckhaults, P., Zhou, S., Kinzler, K. W., Vogelstein, B., and Kern, S. E. (1998) Human Smad3 and Smad4 are sequence-specific transcription activators. *Mol. Cell* **1,** 611–617
28. Hai, T., and Curran, T. (1991) Cross-family dimerization of transcription factors Fos/Jun and ATF/CREB alters DNA binding specificity. *Proc. Natl.*

Acad. Sci. U.S.A. **88,** 3720–3724
29. Kimura, N., Takamatsu, N., Yaoita, Y., and Osamura, R. Y. (2008) Identification of transcriptional regulatory elements in the human somatostatin receptor sst2 promoter and regions including estrogen response element half-site for estrogen activation. *J. Mol. Endocrinol.* **40,** 75–91
30. Nakamura, T., Okuyama, S., Okamoto, S., Nakajima, T., Sekiya, S., and Oda, K. (1995) Down-regulation of the cyclin A promoter in differentiating human embryonal carcinoma cells is mediated by depletion of ATF-1 and ATF-2 in the complex at the ATF/CRE site. *Exp. Cell Res.* **216,** 422–430
31. Hai, T. W., Liu, F., Coukos, W. J., and Green, M. R. (1989) Transcription factor ATF cDNA clones. An extensive family of leucine zipper proteins able to selectively form DNA-binding heterodimers. *Genes Dev.* **3,** 2083–2090
32. Liu, C., Liu, W., Palie, J., Lu, M. F., Brown, N. A., and Martin, J. F. (2002) Pitx2c patterns anterior myocardium and aortic arch vessels and is required for local cell movement into atrioventricular cushions. *Development* **129,** 5081–5091
33. Kettunen, P., Karavanova, I., and Thesleff, I. (1998) Responsiveness of developing dental tissues to fibroblast growth factors. Expression of splicing alternatives of FGFR1, -2, -3, and of FGFR4 and stimulation of cell proliferation by FGF-2, -4, -8, and -9. *Dev. Genet.* **22,** 374–385
34. Colvin, J. S., White, A. C., Pratt, S. J., and Ornitz, D. M. (2001) Lung hypoplasia and neonatal death in *Fgf9*-null mice identify this gene as an essential regulator of lung mesenchyme. *Development* **128,** 2095–2106
35. Lu, M. F., Pressman, C., Dyer, R., Johnson, R. L., and Martin, J. F. (1999) Function of Rieger syndrome gene in left-right asymmetry and craniofacial development. *Nature* **401,** 276–278
36. Zhu, T., and Lobie, P. E. (2000) Janus kinase 2-dependent activation of p38 mitogen-activated protein kinase by growth hormone. Resultant transcriptional activation of ATF-2 and CHOP, cytoskeletal reorganization, and mitogenesis. *J. Biol. Chem.* **275,** 2103–2114
37. Mizuguchi, T., Collod-Beroud, G., Akiyama, T., Abifadel, M., Harada, N., Morisaki, T., Allard, D., Varret, M., Claustres, M., Morisaki, H., Ihara, M., Kinoshita, A., Yoshiura, K., Junien, C., Kajii, T., Jondeau, G., Ohta, T., Kishino, T., Furukawa, Y., Nakamura, Y., Niikawa, N., Boileau, C., and Matsumoto, N. (2004) Heterozygous TGFBR2 mutations in Marfan syndrome. *Nat. Genet.* **36,** 855–860
38. Loeys, B. L., Chen, J., Neptune, E. R., Judge, D. P., Podowski, M., Holm, T., Meyers, J., Leitch, C. C., Katsanis, N., Sharifi, N., Xu, F. L., Myers, L. A., Spevak, P. J., Cameron, D. E., De Backer, J., Hellemans, J., Chen, Y., Davis, E. C., Webb, C. L., Kress, W., Coucke, P., Rifkin, D. B., De Paepe, A. M., Dietz, H. C. (2005) A syndrome of altered cardiovascular, craniofacial, neurocognitive and skeletal development caused by mutations in TGFBR1 or TGFBR2. *Nat. Genet.* **37,** 275–281
39. Loeys, B. L., Schwarze, U., Holm, T., Callewaert, B. L., Thomas, G. H., Pannu, H., De Backer, J. F., Oswald, G. L., Symoens, S., Manouvrier, S., Roberts, A. E., Faravelli, F., Greco, M. A., Pyeritz, R. E., Milewicz, D. M., Coucke, P. J., Cameron, D. E., Braverman, A. C., Byers, P. H., De Paepe, A. M., and Dietz, H. C. (2006) Aneurysm syndromes caused by mutations in the TGF-β receptor. *N. Engl. J. Med.* **355,** 788–798
40. Brooke, B. S., Habashi, J. P., Judge, D. P., Patel, N., Loeys, B., Dietz, H. C., 3rd. (2008) Angiotensin II blockade and aortic-root dilation in Marfan's syndrome. *N. Engl. J. Med.* **358,** 2787–2795
41. Habashi, J. P., Judge, D. P., Holm, T. M., Cohn, R. D., Loeys, B. L., Cooper, T. K., Myers, L., Klein, E. C., Liu, G., Calvi, C., Podowski, M., Neptune, E. R., Halushka, M. K., Bedja, D., Gabrielson, K., Rifkin, D. B., Carta, L., Ramirez, F., Huso, D. L., Dietz, H. C. (2006) Losartan, an AT1 antagonist, prevents aortic aneurysm in a mouse model of Marfan syndrome. *Science.* **312,** 117–121
42. Kalluri, R., and Han, Y. (2008) Targeting TGF-β and the extracellular matrix in Marfan's syndrome. *Dev Cell.* **15,** 1–2
43. Lindsay, E. A. (2001) Chromosomal microdeletions. Dissecting del22q11 syndrome. *Nat. Rev. Genet.* **2,** 858–868
44. Vitelli, F., Morishima, M., Taddei, I., Lindsay, E. A., and Baldini, A. (2002) Tbx1 mutation causes multiple cardiovascular defects and disrupts neural crest and cranial nerve migratory pathways. *Hum. Mol. Genet.* **11,** 915–922
45. Wurdak, H., Ittner, L. M., Lang, K. S., Leveen, P., Suter, U., Fischer, J. A., Karlsson, S., Born, W., and Sommer, L. (2005) Inactivation of TGFβ signaling in neural crest stem cells leads to multiple defects reminiscent of DiGeorge syndrome. *Genes Dev.* **19,** 530–535
46. McKeehan, W. L., Wang, F., and Kan, M. (1998) The heparan sulfate-fibroblast growth factor family. Diversity of structure and function. *Prog. Nucleic Acid Res. Mol. Biol.* **59,** 135–176
47. Riley, B. M., Mansilla, M. A., Ma, J., Daack-Hirsch, S., Maher, B. S., Raffensperger, L. M., Russo, E. T., Vieira, A. R., Dodé, C., Mohammadi, M., Marazita, M. L., and Murray, J. C. (2007) Impaired FGF signaling contributes to cleft lip and palate. *Proc. Natl. Acad. Sci. U.S.A.* **104,** 4512–4517
48. Govindarajan, V., and Overbeek, P. A. (2006) FGF9 can induce endochondral ossification in cranial mesenchyme. *BMC Dev. Biol.* **6,** 7
49. Geske, M. J., Zhang, X., Patel, K. K., Ornitz, D. M., and Stappenbeck, T. S. (2008) Fgf9 signaling regulates small intestinal elongation and mesenchymal development. *Development* **135,** 2959–2968
50. Bellusci, S. (2008) Lung stem cells in the balance. *Nat. Genet.* **40,** 822–824
51. Iwao, K., Inatani, M., Matsumoto, Y., Ogata-Iwao, M., Takihara, Y., Irie, F., Yamaguchi, Y., Okinami, S., and Tanihara, H. (2009) Heparan sulfate deficiency leads to Peters anomaly in mice by disturbing neural crest TGF-β2 signaling. *J. Clin. Invest.* **119,** 1997–2008
52. Holm, T. M., Habashi, J. P., Doyle, J. J., Bedja, D., Chen, Y., van Erp, C., Lindsay, M. E., Kim, D., Schoenhoff, F., Cohn, R. D., Loeys, B. L., Thomas, C. J., Patnaik, S., Marugan, J. J., Judge, D. P., and Dietz, H. C. (2011) Noncanonical TGFβ signaling contributes to aortic aneurysm progression in Marfan syndrome mice. *Science* **332,** 358–361
53. Habashi, J. P., Doyle, J. J., Holm, T. M., Aziz, H., Schoenhoff, F., Bedja, D., Chen, Y., Modiri, A. N., Judge, D. P., and Dietz, H. C. (2011) Angiotensin II type 2 receptor signaling attenuates aortic aneurysm in mice through ERK antagonism. *Science* **332,** 361–365
54. Dudas, M., Kim, J., Li, W. Y., Nagy, A., Larsson, J., Karlsson, S., Chai, Y., and Kaartinen, V. (2006) Epithelial and ectomesenchymal role of the type I TGF-β receptor ALK5 during facial morphogenesis and palatal fusion. *Dev. Biol.* **296,** 298–314
55. Lin, C. R., Kioussi, C., O'Connell, S., Briata, P., Szeto, D., Liu, F., Izpisúa-Belmonte, J. C., and Rosenfeld, M. G. (1999) Pitx2 regulates lung asymmetry, cardiac positioning and pituitary and tooth morphogenesis. *Nature* **401,** 279–282
56. Liu, C., Liu, W., Lu, M. F., Brown, N. A., and Martin, J. F. (2001) Regulation of left-right asymmetry by thresholds of Pitx2c activity. *Development* **128,** 2039–2048
57. Liu, W., Selever, J., Lu, M. F., Martin, J. F. (2003) Genetic dissection of Pitx2 in craniofacial development uncovers new functions in branchial arch morphogenesis, late aspects of tooth morphogenesis and cell migration. *Development* **130,** 6375–6385
58. Kioussi, C., Briata, P., Baek, S. H., Rose, D. W., Hamblet, N. S., Herman, T., Ohgi, K. A., Lin, C., Gleiberman, A., Wang, J., Brault, V., Ruiz-Lozano, P., Nguyen, H. D., Kemler, R., Glass, C. K., Wynshaw-Boris, A., and Rosenfeld, M. G. (2002) Identification of a Wnt/Dvl/beta-Catenin → Pitx2 pathway mediating cell type-specific proliferation during development. *Cell.* **111,** 673–685
59. Hayashi, M., Maeda, S., Aburatani, H., Kitamura, K., Miyoshi, H., Miyazono, K., and Imamura, T. (2008) Pitx2 prevents osteoblastic transdifferentiation of myoblasts by bone morphogenetic proteins. *J. Biol. Chem.* **283,** 565–571
60. Ai, D., Liu, W., Ma, L., Dong, F., Lu, M. F., Wang, D., Verzi, M. P., Cai, C., Gage, P. J., Evans, S., Black, B. L., Brown, N. A., and Martin, J. F. (2006) Pitx2 regulates cardiac left-right asymmetry by patterning second cardiac lineage-derived myocardium. *Dev. Biol.* **296,** 437–449
61. Yoshioka, H., Meno, C., Koshiba, K., Sugihara, M., Itoh, H., Ishimaru, Y., Inoue, T., Ohuchi, H., Semina, E. V., Murray, J. C., Hamada, H., and Noji, S. (1998) Pitx2, a bicoid-type homeobox gene, is involved in a lefty-signaling pathway in determination of left-right asymmetry. *Cell* **94,** 299–305
62. Koziczak, M., Holbro, T., and Hynes, N. E. (2004) Blocking of FGFR signaling inhibits breast cancer cell proliferation through downregulation of D-type cyclins. *Oncogene* **23,** 3501–3508

63. Semina, E. V., Reiter, R., Leysens, N. J., Alward, W. L., Small, K. W., Datson, N. A., Siegel-Bartelt, J., Bierke-Nelson, D., Bitoun, P., Zabel, B. U., Carey, J. C., and Murray, J. C. (1996) Cloning and characterization of a novel bicoid-related homeobox transcription factor gene, RIEG, involved in Rieger syndrome. *Nat. Genet.* **14,** 392–399
64. Martin, D. M., Probst, F. J., Fox, S. E., Schimmenti, L. A., Semina, E. V., Hefner, M. A., Belmont, J. W., and Camper, S. A. (2002) Exclusion of PITX2 mutations as a major cause of CHARGE association. *Am. J. Med. Genet.* **111,** 27–30
65. Espinoza, H. M., Cox, C. J., Semina, E. V., and Amendt, B. A. (2002) A molecular basis for differential developmental anomalies in Axenfeld-Rieger syndrome. *Hum. Mol. Genet.* **11,** 743–753
66. Chai, Y., Ito, Y., and Han, J. (2003) TGF-β signaling and its functional significance in regulating the fate of cranial neural crest cells. *Crit. Rev. Oral. Biol. Med.* **14,** 78 – 88
67. Zhao, H., Oka, K., Bringas, P., Kaartinen, V., and Chai, Y. (2008) TGF-β type I receptor Alk5 regulates tooth initiation and mandible patterning in a type II receptor-independent manner. *Dev. Biol.* **320,** 19 –29